



The molecular structure of matioliite – $\text{NaMgAl}_5(\text{PO}_4)_4(\text{OH})_6 \cdot 2(\text{H}_2\text{O})$ – A pegmatite mineral from Minas Gerais, Brazil

Ricardo Scholz^a, Yunfei Xi^b, Ray L. Frost^{b,*}

^a Geology Department, School of Mines, Federal University of Ouro Preto, Campus Morro do Cruzeiro, Ouro Preto, MG 35400-00, Brazil

^b Discipline of Nanotechnology and Molecular Science, Science and Engineering Faculty, Queensland University of Technology, GPO Box 2434, Brisbane, Queensland 4001, Australia

HIGHLIGHTS

- We have studied the pegmatite phosphate mineral matioliite.
- The composition of the mineral was determined.
- The structure was assessed using vibrational spectroscopic techniques.
- Vibrational spectroscopy proves the existence of hydrogen phosphate and dihydrogen phosphate units in the structure of matioliite.

ARTICLE INFO

Article history:

Received 16 May 2012

Received in revised form 20 September 2012

Accepted 21 September 2012

Available online 22 October 2012

Keywords:

Matioliite

Phosphate

Pegmatite

Infrared spectroscopy

Scanning electron microscopy

Raman spectroscopy

ABSTRACT

Detailed spectroscopic and chemical investigation of matioliite, including infrared and Raman spectroscopy, scanning electron microscopy and electron probe microanalysis has been carried out on homogeneous samples from the Gentil pegmatite, Mendes Pimentel, Minas Gerais, Brazil. The chemical composition is (wt.%): FeO 2.20, CaO 0.05, Na₂O 1.28, MnO 0.06, Al₂O₃ 39.82, P₂O₅ 42.7, MgO 4.68, F 0.02 and H₂O 9.19; total 100.00. The mineral crystallize in the monoclinic crystal system, C2/c space group, with $a = 25.075(1) \text{ \AA}$, $b = 5.0470(3) \text{ \AA}$, $c = 13.4370(7) \text{ \AA}$, $\beta = 110.97(3)^\circ$, $V = 1587.9(4) \text{ \AA}^3$, $Z = 4$.

Raman spectroscopy coupled with infrared spectroscopy supports the concept of phosphate, hydrogen phosphate and dihydrogen phosphate units in the structure of matioliite. Infrared and Raman bands attributed to water and hydroxyl stretching modes are identified. Vibrational spectroscopy adds useful information to the molecular structure of matioliite.

© 2012 Elsevier B.V. All rights reserved.

1. Introduction

Matioliite is a rare hydrated basic aluminum phosphate mineral with sodium and magnesium, and shows general chemical formula expressed by $\text{NaMgAl}_5(\text{PO}_4)_4(\text{OH})_6 \cdot 2(\text{H}_2\text{O})$. It was first described from the Gentil mine, a granitic pegmatite located at Mendes Pimentel, Minas Gerais, Southeastern Brazil. Matioliite forms a solid solution with burangaite – $(\text{Na,Ca})(\text{Fe,Mg})\text{Al}_5(\text{PO}_4)_4(\text{OH})_6 \cdot 2(\text{H}_2\text{O})$ [1], the Fe²⁺ end member of a Mg–Fe series. In addition to burangaite, matioliite is isostructural with dufrénite and natrodufrénite, and crystallize in the monoclinic crystal system, C2/c space group with $a = 25.075(1) \text{ \AA}$, $b = 5.0470(3) \text{ \AA}$, $c = 13.4370(7) \text{ \AA}$, $\beta = 110.97(3)^\circ$,

$V = 1587.9(4) \text{ \AA}^3$, $Z = 4$ [2]. After the type locality, other two occurrences are known in Eureka Co. in Nevada, USA [3] and Hochgösch in Carinthia, Austria [4].

Matioliite occurs as secondary phosphate mineral in lithium bearing pegmatites with primary montebrasite and triphylite and is associated with brazilianite, gormanite, fluorapatite and crandallite, forming a paragenesis in a phosphate rich hydrothermal system [5,6].

According to Selway et al. [7], the fundamental building block of the structure of burangaite, as well as matioliite, is a face-sharing triplet of octahedra $[\text{Al}\chi_6\text{--Mg}\chi_6\text{--Al}\chi_6]$ corner linked to two $\text{Al}\chi_6$ octahedra and two PO_4 tetrahedra, where χ is an unspecified anionic species. This block is polymerized parallel to the c -axis to form dense slabs in the $\{100\}$ plane. Alternating $\text{Al}\chi_6$ octahedra and $\text{Na}\chi_8$ polyhedra form a chain parallel to the c -axis, and the dense slab and chain alternate along the a -axis. Al occurs at three symmetrically distinct sites coordinated in an octahedral arrangement. The Al1 site is coordinated by two O anions, two (OH) groups and two (H₂O) groups. The Al3 site is coordinated by three O

* Corresponding author. Tel.: +61 7 3138 2407; fax: +61 7 3138 1804.

E-mail addresses: r_scholz_br@yahoo.com (R. Scholz), r.frost@qut.edu.au (R.L. Frost).

anions and three (OH) groups. The Al4 site is coordinated by four O anions and two (OH) groups. Phosphorus occurs at two symmetrically distinct sites, each coordinated by four O in a tetrahedral arrangement. The Na site is coordinated by six O anions and two (H₂O) groups to form a cubic antiprism. Mg atom is coordinated by four O anions and two (OH) groups in an octahedral arrangement.

In recent years, the application of spectroscopic techniques to understand the structure of phosphates is increasing, with special attention to Al phosphates [8–12]. Farmer [13] divided the vibrational spectra of phosphates according to the presence, or absence of water and hydroxyl units in the minerals. In aqueous systems, Raman spectra of phosphate oxyanions show a symmetric stretching mode (ν_1) at 938 cm⁻¹, the antisymmetric stretching mode (ν_3) at 1017 cm⁻¹, the symmetric bending mode (ν_2) at 420 cm⁻¹ and the ν_4 mode at 567 cm⁻¹ [14–16]. The value for the ν_1 symmetric stretching vibration of PO₄ units as determined by infrared spectroscopy was given as 930 cm⁻¹ (augelite), 940 cm⁻¹ (wavellite), 970 cm⁻¹ (rockbridgeite), 995 cm⁻¹ (dufrénite) and 965 cm⁻¹ (beraunite). The position of the symmetric stretching vibration is mineral dependent and a function of the cation and crystal structure. The fact that the symmetric stretching mode is observed in the infrared spectrum affirms a reduction in symmetry of the PO₄ units.

The value for the ν_2 symmetric bending vibration of PO₄ units as determined by infrared spectroscopy was given as 438 cm⁻¹ (augelite), 452 cm⁻¹ (wavellite), 440 and 415 cm⁻¹ (rockbridgeite), 455, 435 and 415 cm⁻¹ (dufrénite) and 470 and 450 cm⁻¹ (beraunite). The observation of multiple bending modes provides an indication of symmetry reduction of the PO₄ units. This symmetry reduction is also observed through the ν_3 antisymmetric stretching vibrations. Augelite shows infrared bands at 1205, 1155, 1079 and 1015 cm⁻¹ [8]; wavellite at 1145, 1102, 1062 and 1025 cm⁻¹; rockbridgeite at 1145, 1060 and 1030 cm⁻¹; dufrénite at 1135, 1070 and 1032 cm⁻¹; and beraunite at 1150, 1100, 1076 and 1035 cm⁻¹.

In this work, spectroscopic investigation of a monomineral matioliite sample from the type locality in Brazil has been carried out. The analysis includes spectroscopic characterization of the structure with infrared and Raman spectroscopy.

2. Methods

2.1. Sample preparation

Light blue to greenish blue matioliite crystals were collected from the type locality, a granitic pegmatite named Gentil mine. The sample was incorporated in the collection of the Geology Department of the Federal University of Ouro Preto, Minas Gerais, Brazil, with sample code SAA-070. The crystals were hand selected

from a sample in association with brazilianite and crandallite (Fig. 1).

The matioliite crystals were phase analyzed by X-ray diffraction and shows the following crystallographic parameters: $a = 25.012(3)$ Å, $b = 5.0368(7)$ Å, $c = 13.4027(16)$ Å, $\beta = 110.937(8)^\circ$, $V = 1577.0(4)$ Å³, $C2/c$, $Z = 4$, showing similar of those published by Atencio et al. [2]. Two single crystals were prepared in polyester resin for quantitative chemical analysis, with five points analyzed in each crystal. The polishment was done in the sequence of 9 µm, 6 µm and 1 µm diamond paste MetaDI® II Diamond Paste – Buhler, using water as a lubricant, with a semi-automatic Mini-Met® 1000 Grinder–Polisher–Buehler.

2.2. Scanning electron microscopy (SEM)

Matioliite samples were coated with a thin layer of evaporated carbon. Secondary Electron and Backscattering images were obtained using a JEOL-JSM840A scanning electron microscope from the Physics Department of the Federal University of Minas Gerais, Belo Horizonte. Qualitative chemical analyses by SEM in the EDS mode were produced to support the mineral characterization and determine the elements to be analyzed by Electron probe microanalysis.

2.3. Electron probe microanalysis (EPMA)

EPMA was carried in a selection of two single crystals, with the performance of five spots per crystal. The chemical analysis was carried out with a Jeol JXA8900R spectrometer from the Physics Department of the Federal University of Minas Gerais, Belo Horizonte. For each selected element was used the following standards: Fe and Mg – olivine, Mn – rhodonite, P and Ca – Apatite Artimex, Na – Albite, Al – Corundum and F – Fluorite. The epoxy embedded matioliite samples were coated with a thin layer of evaporated carbon. The electron probe microanalysis in the WDS (wavelength dispersive spectrometer) mode was obtained at 15 kV accelerating voltage and beam current of 10 nA.

2.4. Raman microprobe spectroscopy

Crystals of matioliite were placed on a polished metal surface on the stage of an Olympus BHSM microscope, which is equipped with 10×, 20×, and 50× objectives. The microscope is part of a Renishaw 1000 Raman microscope system, which also includes a monochromator, a filter system and a CCD detector (1024 pixels). The Raman spectra were excited by a Spectra-Physics model 127 He–Ne laser producing highly polarized light at 633 nm and collected at a nominal resolution of 2 cm⁻¹ and a precision of ± 1 cm⁻¹ in the range between 200 and 4000 cm⁻¹. Repeated acquisitions on the crystals using the highest magnification (50×) were accumulated to improve the signal to noise ratio of the spectra. The spectra were collected over night. Raman Spectra were calibrated using the 520.5 cm⁻¹ line of a silicon wafer. The Raman spectrum of at least 10 crystals was collected to ensure the consistency of the spectra.

2.5. Infrared spectroscopy

Infrared spectra were obtained using a Nicolet Nexus 870 FTIR spectrometer with a smart endurance single bounce diamond ATR cell. Spectra over the 4000–525 cm⁻¹ range were obtained by the co-addition of 128 scans with a resolution of 4 cm⁻¹ and a mirror velocity of 0.6329 cm/s. Spectra were co-added to improve the signal to noise ratio. The infrared spectra are given in the supplementary information.

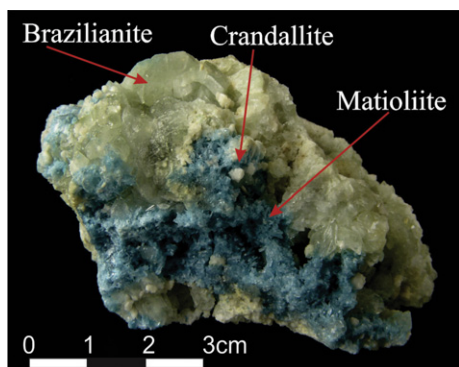


Fig. 1. Matioliite crystals in association with brazilianite and crandallite.

Spectral manipulation such as baseline correction/adjustment and smoothing were performed using the Spectralcalc software package GRAMS (Galactic Industries Corporation, NH, USA). Band component analysis was undertaken using the Jandel 'Peakfit' software package that enabled the type of fitting function to be selected and allows specific parameters to be fixed or varied accordingly. Band fitting was done using a Lorentzian–Gaussian cross-product function with the minimum number of component bands used for the fitting process. The Gaussian–Lorentzian ratio was maintained at values greater than 0.7 and fitting was undertaken until reproducible results were obtained with squared correlations of r^2 greater than 0.995.

3. Results and discussion

3.1. Chemical characterization

The SEM images of a matioliite crystals studied in this work are shown in Fig. 2. The image presented in the Fig. 2a was obtained with secondary electrons and shows a brazilianite crystal up to 3.0 mm in length, with matioliite growing on the surface. The matioliite crystals are organized in radiating groups of simple prismatic monoclinic crystals of about 0.2 mm in length. The mineral association suggests that matioliite grows after the crystallization of brazilianite. Fig. 2b was obtained with backscattered electrons and shows a single crystal of matioliite, with monoclinic prismatic to tabular form with up to 0.3 mm in length in the crystallographic c axis.

The quantitative chemical analysis of matioliite is presented in Table 1. The chemical composition indicates an intermediate member of the burangaite–matioliite series with predominance of the matioliite end-member. The results show variable amounts of Fe and Ca, which replaces partially Mg and Na, respectively.

3.2. Spectroscopy

The Raman spectrum of matioliite in the 100–4000 cm^{-1} region is displayed in Fig. 3a. This figure reports the position of the bands and their relative intensity. It is noted that there are regions in the spectrum where no intensity is observed. Therefore, the spectrum is subdivided into sections in subsequent figures so that more detailed assessment of the spectra can be made. In a similar way, the infrared spectrum of matioliite in the 500–4000 cm^{-1} region is reported in Fig. 1b. The spectrum is not shown below 500 cm^{-1} . The reason is that we are using a reflectance technique

Table 1

Chemical composition of matioliite from Gentil pegmatite (mean of 10 electron microprobe analyses). H_2O calculated by difference.

Constituent	wt.%	Range	Probe standard
MgO	4.68	3.61–5.57	Olivine
FeO	2.20	1.02–3.85	Olivine
MnO	0.06	0.03–0.15	Rhodonite
CaO	0.05	0.00–0.21	Apatite Artimex
Na_2O	1.28	0.92–1.65	Albite
Al_2O_3	39.82	38.39–40.83	Corundum
P_2O_5	42.7	41.72–43.78	Apatite Artimex
F	0.02	0.01–0.23	Fluorite
H_2O	9.19	Calculated by difference	
Total	100.00		

is being used and the ATR cell absorbs all incident radiation below 500 cm^{-1} . In a similar fashion to the Raman spectrum, the infrared spectrum is divided into sections depending upon the types of vibrations being observed. The Raman spectrum of matioliite in the 800–1400 cm^{-1} region is reported in Fig. 4a. The infrared spectrum of matioliite in the 500–1300 cm^{-1} region is reported in Fig. 4b.

The Raman spectrum in the 800–1400 cm^{-1} region is dominated by two very sharp bands of almost equal intensity at 1025 and 1048 cm^{-1} . These two bands are assigned to the $\nu_1 \text{PO}_4^{3-}$ symmetric stretching mode. The observation of two symmetric stretching modes supports the concept that there are two non-equivalent phosphate units in the structure of matioliite. The higher wave-number bands at 1068, 1104 are assigned to the $\nu_3 \text{PO}_4^{3-}$ antisymmetric stretching mode. The Raman band at 985 cm^{-1} is considered to be due to HPO_4^{2-} units.

Galy [17] first studied the polarized Raman spectra of the H_2PO_4^- anion. Choi et al. [18] reported the polarization spectra of NaH_2PO_4 crystals. Casciani and Condrate [19] published spectra on brushite and monetite together with synthetic anhydrous monocalcium phosphate $[\text{Ca}(\text{H}_2\text{PO}_4)_2]$, monocalcium dihydrogen phosphate hydrate $(\text{Ca}(\text{H}_2\text{PO}_4)_2 \cdot \text{H}_2\text{O})$ and octacalcium phosphate $[\text{Ca}_8\text{H}_2(\text{PO}_4)_6 \cdot 5\text{H}_2\text{O}]$. These authors determined band assignments for $\text{Ca}(\text{H}_2\text{PO}_4)_2$ and reported bands at 1002 and 1011 cm^{-1} as POH and PO stretching vibrations, respectively. The two Raman bands at 1139 and 1165 cm^{-1} are attributed to both the HOP and PO antisymmetric stretching vibrations. Casciani and Condrate [19] tabulated Raman bands at 1132 and 1155 cm^{-1} and assigned these bands to P–O symmetric and the P–O antisymmetric stretching vibrations. Raman spectroscopy identifies the presence of phosphate,

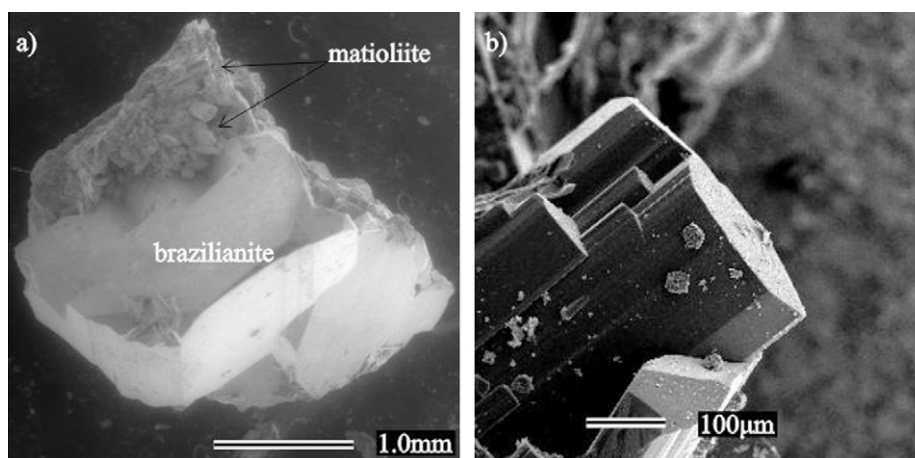


Fig. 2. (a) Secondary electron imaging with SEM of matioliite crystals in association with brazilianite and (b) backscattered electron image of matioliite single crystal showing monoclinic prismatic form. Crystal up to 500 μm .

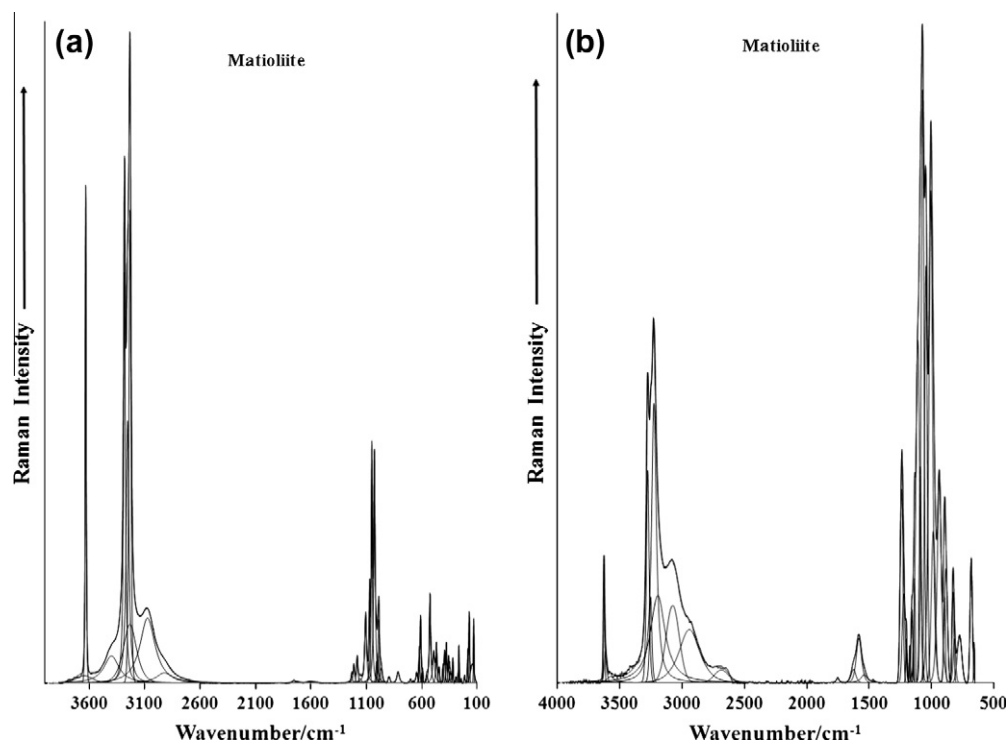


Fig. 3. (a) Raman Spectrum of matioliite the 100–4000 cm^{-1} region and (b) infrared spectrum of matioliite in the 500–4000 cm^{-1} region.

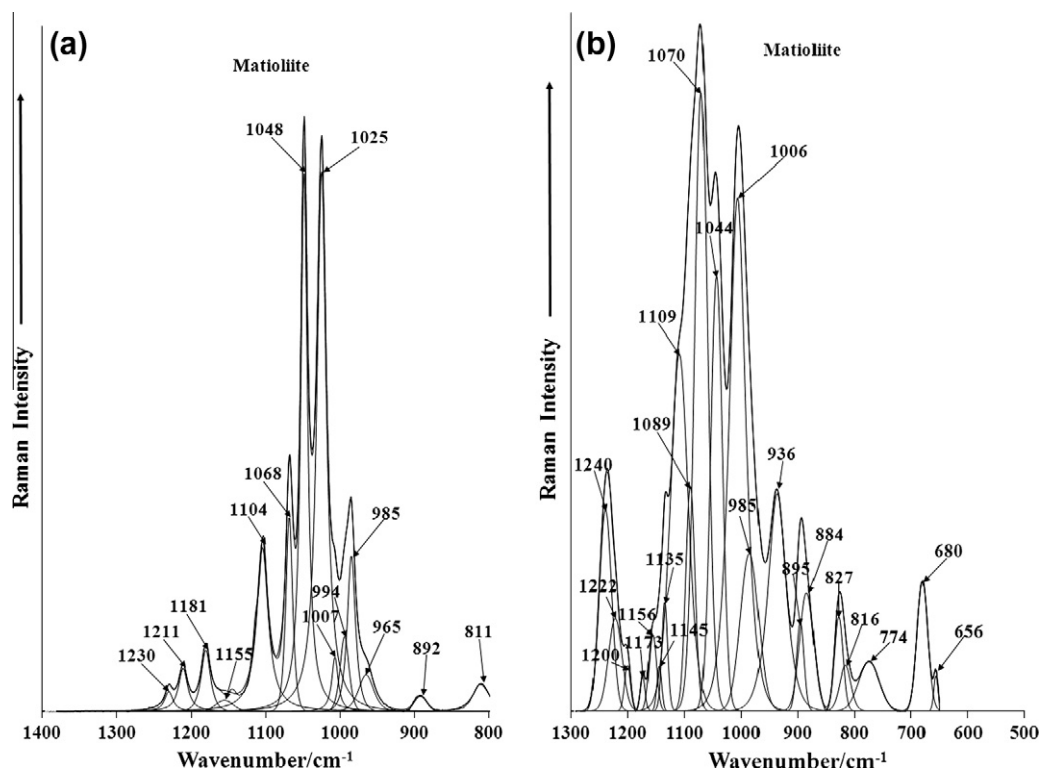


Fig. 4. (a) Raman spectrum of matioliite in the 800–1400 cm^{-1} region and (b) infrared spectrum of matioliite in the 500–1300 cm^{-1} .

hydrogen phosphate and dihydrogen phosphate units. The infrared spectrum (Fig. 4b) show a complex set of overlapping bands. The two infrared bands at 985 and 1006 cm^{-1} are attributed to the ν_1 PO_4^{3-} symmetric stretching modes. The intense bands at 1044, 1070, 1109 and 1135 cm^{-1} are assigned to the ν_3 PO_4^{3-} antisymmetric stretching modes.

The Raman spectra of matioliite in the 300–800 cm^{-1} and in the 100–300 cm^{-1} region are shown in Fig. 5a and b respectively. The spectra show the complexity in harmony with the spectrum reported in Fig. 4a and b. The Raman spectral region shown in Fig. 6a represents the bending region of the phosphate units. A set of Raman bands at 590, 599, 609 and 620 cm^{-1} are assigned

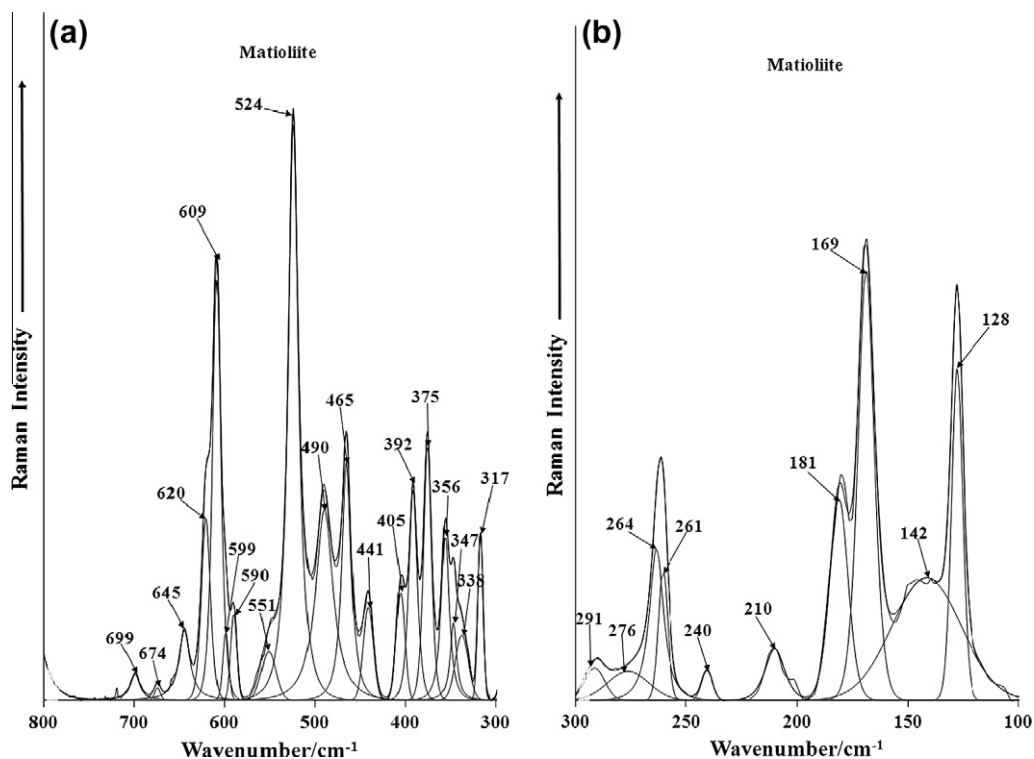


Fig. 5. (a) Raman spectra of matoiliite in the 300–800 cm^{-1} and (b) Raman spectra of matoiliite in the 100–300 cm^{-1} region.

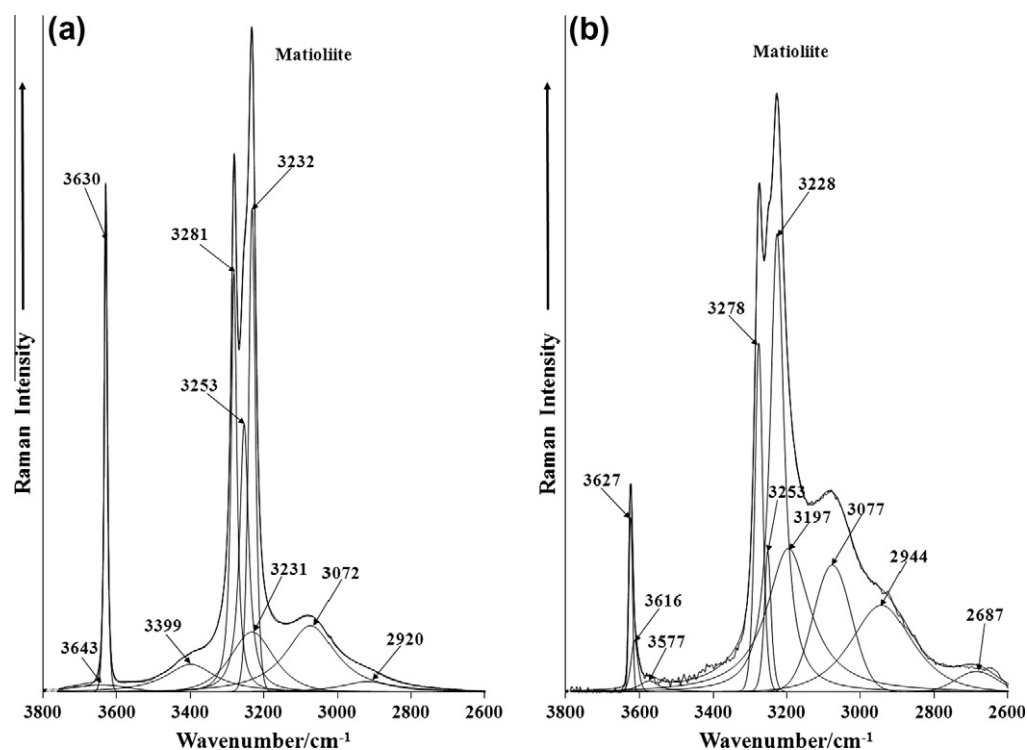


Fig. 6. (a) Raman spectrum of matoiliite in the 2600–3800 cm^{-1} region and (b) infrared spectrum of matoiliite in the 2600–3800 cm^{-1} region.

to the ν_4 out of plane bending modes of the PO_4 , HPO_4 and H_2PO_4 units. The Raman spectrum of NaH_2PO_4 shows Raman bands at 526, 546 and 618 cm^{-1} (this work). The infrared spectrum of matoiliite (Fig. 4b) shows two bands at 656 and 680 cm^{-1} and is assigned to this vibrational mode. In the infrared spectrum of dittmarite ($(\text{NH}_4)\text{MgPO}_4 \cdot \text{H}_2\text{O}$) bands are observed at 635 and

656 cm^{-1} and are assigned to the PO_4^{3-} ν_4 bending mode. Raman bands are observed at 441, 465, 490 and 524 cm^{-1} . These bands are attributed to the ν_2 PO_4 , HPO_4 and H_2PO_4 bending modes. The Raman spectrum of NaH_2PO_4 shows Raman bands at 460 and 482 cm^{-1} which are assigned to this vibrational mode. A set of Raman bands is observed at 317, 338, 347, 356, 375, 392 and

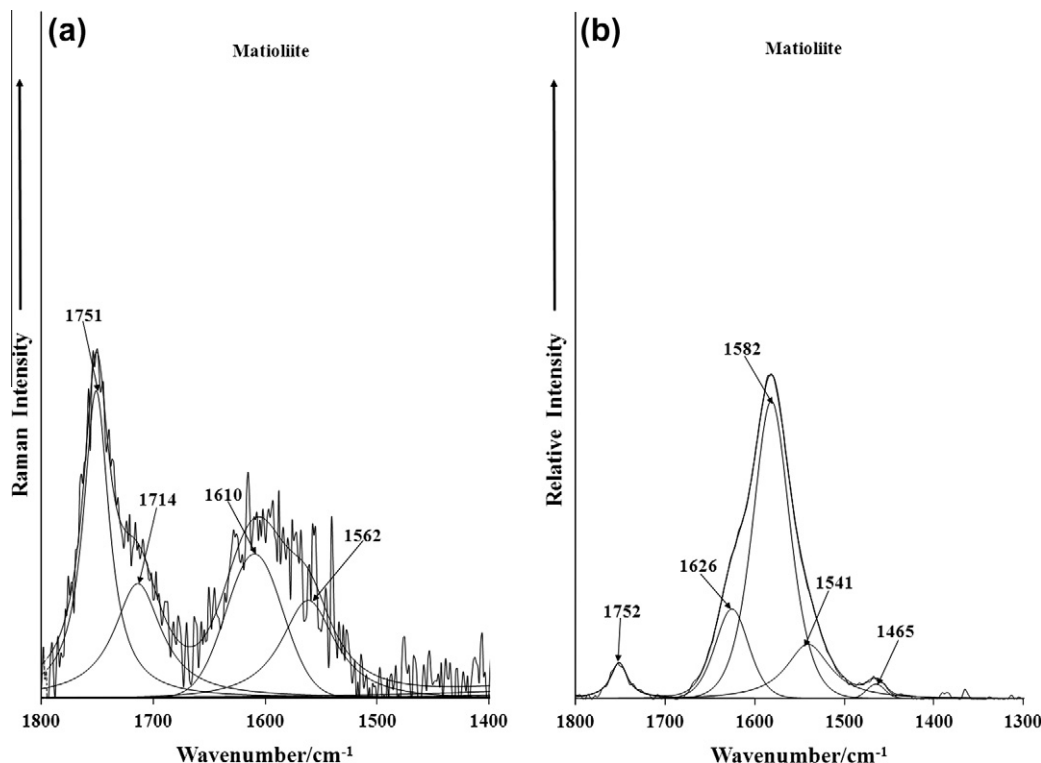


Fig. 7. (a) Raman spectrum of matioliite in the 1400–1800 cm^{-1} region and (b) infrared spectrum of matioliite in the 1300–1800 cm^{-1} region.

405 cm^{-1} . These bands are considered to be due to metal–oxygen stretching vibrations. Strong Raman bands are observed in the far low wavenumber region at 128, 169, 181, 261 and 264 cm^{-1} . These bands are described as lattice vibrations.

The Raman spectrum of matioliite and the infrared spectrum in the 2600–3800 cm^{-1} region are illustrated in Fig. 6a and b. Raman peaks are observed at 3232, 3281 and 3630 cm^{-1} ; the first two peaks are assigned to water stretching vibrations and the latter to OH stretching bands. Other low intensity Raman bands are observed at 2920, 3072, 3231 and 3399 cm^{-1} . These bands show much greater intensity in the infrared spectrum. Two intense infrared bands are observed at 3228 and 3278 cm^{-1} and are assigned to water stretching vibrations. The infrared band at 3627 cm^{-1} is attributed to OH unit stretching vibration. Other infrared bands are observed at 2678, 2944, 3077, 3197 and 3525 cm^{-1} . The observation of two distinct Raman stretching vibrations for matioliite suggests that there are two distinct non-equivalent water molecules in the structure. This concept is supported by the multiple infrared bands. In comparison, only a single OH stretching vibration is observed in both the infrared and Raman spectrum, thus indicating that all the OH units are spectroscopically identical.

The Raman spectrum in the 1400–1800 cm^{-1} and the infrared spectrum in the 1300–1800 cm^{-1} are reported in Fig. 7a and b respectively. A low intensity Raman band is observed at 1610 cm^{-1} and is attributed to the water bending mode. The band shows much greater intensity in the infrared spectrum and is observed as a band at 1626 cm^{-1} . The Raman spectrum shows a band at 1751 cm^{-1} with a shoulder band at 1714 cm^{-1} . These bands are also reflected in the infrared spectrum with the band observed at 1752 cm^{-1} . These bands are attributed to overtone or combination bands. In the infrared spectrum bands are observed at 1465, 1541 and 1582 cm^{-1} .

4. Conclusions

Matioliite is a rare hydrated basic aluminum phosphate mineral with sodium and magnesium and forms a solid solution with burangaite where magnesium is substituted by iron. A sample of matioliite from the type locality was characterized by EPMA, SEM and Raman and infrared spectroscopic measurements. Chemical composition shows an intermediate member in the solid solution with predominance of the matioliite end-member.

Acknowledgements

The financial and infra-structure support of the Discipline of Nanotechnology and Molecular Science, Science and Engineering Faculty of the Queensland University of Technology, is gratefully acknowledged. The Australian Research Council (ARC) is thanked for funding the instrumentation. R. Scholz thanks to FAPEMIG – Fundação de Amparo à Pesquisa do Estado de Minas Gerais (Grant No. CRA-APQ-03998-10).

References

- [1] O. von Knorring, M. Lehtinen, Th.G. Sahama, *Bull. Geol. Soc. Finland* 49 (1977) 33.
- [2] D. Atencio, J.M.V. Coutinho, Y.P. Mascarenhas, J.A. Ellena, *Am. Mineral.* 91 (2006) 1932.
- [3] M. Jensen, J.C. Rota, E.E. Foord, *Mineral. Rec.* 26 (1995) 449.
- [4] F. Walter, K. Ettinger, *Carinthia II* (191) (2001) 149.
- [5] M.L.S.C. Chaves, R. Scholz, D. Atencio, J. Karfunkel, *Geociências* 24 (2005) 143 (in Portuguese).
- [6] M.L.S.C. Chaves, R. Scholz, *Revista Escola de Minas* 61 (2008) 141.
- [7] J.B. Selway, M.A. Cooper, F.C. Hawthorne, *Can. Mineral.* 35 (1997) 1515.
- [8] R.L. Frost, M.L. Weier, K.L. Erickson, L. Kristy, O. Carmody, S. Mills, *J. Raman Spectrosc.* 35 (2004) 1047.
- [9] L.N. Dias, M.V.B. Pinheiro, R.L. Moreira, K. Krambrock, K. Guedes, L.A.D. Menezes Filho, J. Karfunkel, J. Schnellrath, R. Scholz, *Am. Mineral.* 96 (2011) 42.

- [10] R.L. Frost, Y. Xi, S.J. Palmer, R. Pogson, *Spectrochim. Acta A: Mol. Biomol. Spectrosc.* 82 (2011) 461.
- [11] R.L. Frost, Y. Xi, S.J. Palmer, *J. Mol. Struct.* 1001 (2011) 56.
- [12] R.L. Frost, Y. Xi, *J. Mol. Struct.* 1010 (2012) 179.
- [13] V.C. Farmer, *Mineralogical Society Monograph 4, The Infrared Spectra of Minerals*, 1974.
- [14] R.L. Frost, W. Martens, P.A. Williams, J.T. Kloprogge, *Mineral. Mag.* 66 (2002) 1063.
- [15] R.L. Frost, W.N. Martens, T. Kloprogge, P.A. Williams, *Neues Jahrbuch für Mineralogie, Monatshefte* 11 (2002) 481.
- [16] R.L. Frost, P.A. Williams, W. Martens, J.T. Kloprogge, P. Leverett, *J. Raman Spectrosc.* 33 (2002) 260.
- [17] A. Galy, *J. Phys – Paris* 12 (1951) 827.
- [18] B.K. Choi, M.N. Lee, J.J. Kim, *J. Raman Spectrosc.* 20 (1989) 11.
- [19] F.S. Casciani, R.A. Condrate Sr., *Proceedings – International Congress on Phosphorus Compounds*, 2nd, 1980, pp. 175.